IEEE Robotics and Automation Letters (RA-L) paper, presented at ICRA 2023, London, UK. Cite as RA-L paper.

Hybrid Half-Gaussian Selectively Adaptive Fuzzy Control of an Actuated Ankle–Foot Orthosis

Huiseok Moon[1], Roshni Maiti[2], Kaushik Das Sharma[2], Yacine Amirat[1], Patrick Siarry[1] and Samer Mohammed[1]

***Abstract*—To control an actuated ankle–foot orthosis (AAFO) during walking, a selectively adaptive hybrid fuzzy control employing particle-swarm optimization was used in conjunction with a Lyapunov-theory-based adaptive fuzzy-logic control. Adaptation (a computationally expensive process) was performed only when the tracking error exceeded a certain half-Gaussian function. The stability of the overall closed-loop system was proved using Lyapunov theory. The proposed control strategy was verified both by simulations and by experiments with five healthy subjects. The proposed control strategy significantly reduced both tracking error and required control torque when compared to other competing control schemes.**

***Index Terms*—Rehabilitation Robotics, Robust/Adaptive Control, Neural and Fuzzy Control, Wearable Robotics**

I. Introduction

FOOT-DROP—insufficient clearance by the forefoot during the swing phase of walking—is a symptom sometimes exhibited by patients who have experienced spinal-cord injury (SCI) or a stroke and have entirely or partially lost control of their lower-limb muscles and ankle joint [1]. In some cases, such patients are completely unable to initiate a desired movement of the affected limb; in others, they are able to lift their foot only to a limited extent while walking. In both cases, movement coordination and posture balance are affected, increasing the fall risk. Conventional therapy consists of repetitive manual exercises, tasks that are often painful and may demand considerable physical effort by both patients and clinical staff [2]. Other techniques are also used to compensate for walking deficiencies: functional electrical stimulation (FES) [3], the use of passive orthoses, and (more recently) the use of wearable actuated devices, also known as actuated ankle–foot orthoses (AAFOs) [4]–[7]. An AAFO improves the patient's walking abilities by providing functional assistance in both directions of the sagittal plan (i.e., dorsiflexion and plantarflexion during gait. Several control strategies have been proposed in the literature for using AAFOs to assist paretic patients, among them torque control (which provides constant or gait-phase dependent torque [4]) and control strategies that adapt dynamic parameters (such as the stiffness, inertia, or impedance of the coupled human–exoskeleton system) to the detected gait phase [5]–[7]. Impedance-based controllers that do not require a predefined trajectory have also been studied; however, with these, residual voluntary efforts are needed to initiate movements [8]. If the patient lacks the ability to perform a given movement even partially, approaches based on trajectory tracking would be more advantageous. Therefore, in most cases, controllers have been designed to limit the tracking error with respect to a predefined reference trajectory, often one extracted from standard walking profiles of healthy subjects [9], [10].

Physical interaction between the wearer and the AAFO during walking results in a highly nonlinear system with unknown, time-varying disturbances and model uncertainties. It has been shown in the literature that these can be modelled and controlled utilizing adaptive fuzzy-logic controllers [11], [12]. Recently, there have been attempts to optimize the design of such controllers using modern techniques [13], [14]. For example, in [15], weight learning based on particle swarm optimization (PSO) was implemented in a fuzzy controller, but the performance with unknown time-varying parameters was poor. To obtain an optimal stable adaptive fuzzy-logic controller (AFLC) for AAFO applications, global PSO and a Lyapunov-based local-search technique have been employed in tandem [16]. However, coping with changes in the operational environment, such as those that occur when walking, requires adaptation of the controller parameters throughout the process. This increases the control energy and is not practical for a compact wearable robotic device.

In this paper, a half-Gaussian selective-adaptation strategy is adopted to find an optimal compromise between the tracking errors and the control energy consumption due to the adaptation process. PSO has been hybridized with the Lyapunov theory to design a stochastic-optimization-based hybrid half-Gaussian selectively adaptive (HGSA) stable fuzzy controller. (In [17], a PSO-based selectively adaptive fuzzy controller was implemented, but the selection was dependent upon the integral absolute error (IAE). By contrast, in this work, a novel half-Gaussian selection process is applied.) The proposed control strategy is applied to an AAFO for controlling plantarflexion and dorsiflexion of the ankle joint during walking. Positions of the output singletons of fuzzy controller are at first selected by PSO and then concurrently adapted following the HGSA strategy. The adaptation is selective in that it is not required continually, but only when time-varying parameters such as heel-strike moment appear in the system. When such disturbances are absent, e.g., during the swing phase, the use of adaptation would unnecessarily increase the computational

Manuscript received: February 22, 2022; Revised: May, 19, 2022; Accepted: June, 28, 2022.

This paper was recommended for publication by Editor Jee-Hwan Ryu upon evaluation of the Associate Editor and Reviewers' comments.

[1]H. Moon, Y. Amirat, P. Siarry and S. Mohammed are with Univ Paris Est Créteil, LISSI, F-94400 Vitry, France. (*Corresponding author: S. Mohammed* e-mail: samer.mohammed@u-pec.fr)

[2]R. Maiti and K. Das Sharma are with Systems and Control Lab, Department of Applied Physics, University of Calcutta, 92, APC Road, Kolkata-700009, India

Digital Object Identifier (DOI): see top of this page.

IEEE Robotics and Automation Letters (RA-L) paper, presented at ICRA 2023, London, UK. Cite as RA-L paper.

burden as well as the required control energy. The stability of the overall closed-loop system with the AAFO is guaranteed using the Lyapunov theory. In summary, the novelty of the proposed approach lies in the development of a selectively adaptive stable fuzzy controller that is capable of producing an adequate control signal for an AAFO confronted with time-varying uncertainties and disturbances. The contributions of this paper are as follows:

a. A novel half-Gaussian selectivity strategy of adaptation is used for designing a stable hybrid fuzzy controller able to cope with time-varying uncertainties and disturbances.
b. Simulations and real-life experiments with healthy subjects show that the trajectory-tracking performance of the proposed controller equals or surpasses that of other existing systems.
c. The proposed fuzzy controller reduces computational effort and required control energy, enabling successful operation of the AAFO system in the activities of daily life.

The rest of the paper is organized as follows: Section II presents a description of the experimental AAFO system. Section III details the design of the proposed hybrid stable AFLC. In section IV, the results of simulations and experiments with the proposed hybrid adaptation strategies are presented and analyzed. Section V concludes the paper.

II. Actuated Ankle–Foot Orthosis Dynamics

The AAFO-system dynamics depends on the physical parameters of the subject. The orthosis's movement is synchronized with the wearer's leg through the straps of the thigh, shank, and shoes. The AAFO system considered in this paper consists of a passive brace at the knee joint and a brushless DC (BLDC) motor-based actuated joint at the ankle level in the sagittal plane. As shown in Fig. 1a, the foot's coordinate system $F = (x^{foot}, y^{foot})$ has abscissa x^{foot} with the positive direction increasing distally along the foot; the origin is located at the center of the ankle joint. In the AAFO coordinate system, dorsiflexion corresponds to a positive (clockwise) rotation around the ankle joint. Angular speed and angular acceleration are denoted by $\dot{\phi}$ and $\ddot{\phi}$ respectively.

The objective of this paper is to use a direct adaptive fuzzy control scheme as the basis of a control strategy that remains stable under the nonlinearities present in a coupled human–AAFO system, as well as the potential external disturbances that occur during walking. The system dynamics is given by [6]:

$$J\ddot{\phi} = \tau_f + \tau_a + \tau_s + \tau_r + \tau_{gravity} + \tau_h + u_1, \quad (1)$$

where J is the moment of inertia of the coupled human–AAFO system, τ_f expresses the solid and viscous friction torques, τ_a is the torque induced by the linear movement of the foot, τ_s is the joint-stiffness torque of the system, τ_r is the net torque due to ground-reaction forces (GRF), $\tau_{gravity}$ is the gravitational torque, τ_h is the interaction torque generated by the wearer, and u_1 is the control torque generated by the AAFO when uncertainties are not considered explicitly. All torques are considered to be positive in the dorsiflexion direction.

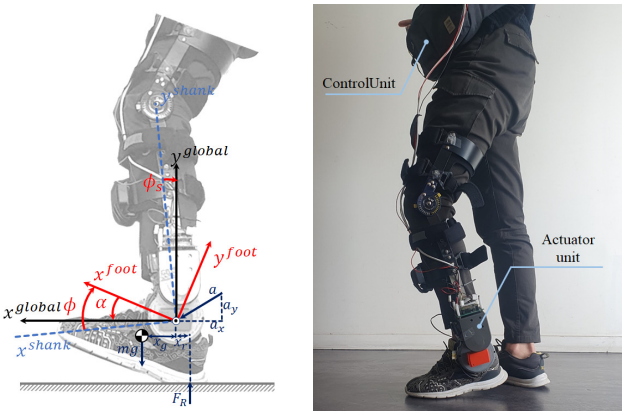

(a) (b)

Fig. 1. Actuated ankle–foot orthosis (AAFO) system (a) Showing global and foot coordinate systems and ground-reaction force F_R. (b) System configuration: Healthy subject wearing the AAFO.

The various torques in (1) can be expanded as:

$$\begin{aligned} &\tau_f = -k_{fs}\text{sign}\dot{\phi} - k_{fv}\dot{\phi}, \tau_s = -k_s(\phi - \phi_r), \\ &\tau_a = -k_a(a_y \cos\alpha – a_x \sin\alpha), \\ &\tau_r = -k_{GRF}(x_R F_R)\cos\alpha, \tau_{gravity} = -k_g \cos\alpha, \end{aligned} \quad (2)$$

where k_{fs}, k_{fv}, k_a, k_s, k_{GRF} and k_g are the coefficients of solid and viscous friction, the system's linear acceleration torque, the system's stiffness, the GRF, and the system's gravity torque. The last of these is expressed as $k_g = mgx_g$, where m is the mass of the system (e.g., the mass of the patient's foot and that of the orthosis), g is the acceleration due to gravity, and x_g is the distance from the ankle joint to the foot's center of mass (COM). F_R is the net GRF applied to the COM of the foot at a distance x_R from the center of the ankle joint in the x^{foot} direction; a_x and a_y are the horizontal and vertical linear accelerations in global frame; and $\alpha = \phi_s - \phi$, where ϕ_s denotes the angle between the shank and the vertical axis, and ϕ_r denotes the ankle-joint angle at the foot's rest position (e.g., standing posture).

The system's endogenous and exogenous torques are considered as disturbances to the system. Therefore, the AAFO system of (2) can be provided as follows:

$$J\ddot{\phi} + B\dot{\phi} + C\phi = u_1 + d(t) \quad (3)$$

If the parametric uncertainties present with J, B and C are given as $\Delta J, \Delta B$ and ΔC respectively then the equation can be rewritten as:

$$(J + \Delta J)\ddot{\phi} + (B + \Delta B)\dot{\phi} + (C + \Delta C)\phi = u + d(t) \quad (4)$$

Which again can be written as:

$$J\ddot{\phi} + B\dot{\phi} + C\phi = u + \xi(t) + d(t), \quad (5)$$

where $\xi(t) = -\Delta J\ddot{\phi} - \Delta B\dot{\phi} - \Delta C\phi$, u is the control signal required when uncertainties present in the system, and

$$\begin{aligned} d(t) =& \tau_h - k_{fs}\text{sign}\dot{\phi} - k_g \cos\alpha + k_s\phi_r \\ &- k_a(a_y \cos\alpha - a_x \sin\alpha) - k_{GRF}(x_R F_R)\cos\alpha. \end{aligned} \quad (6)$$

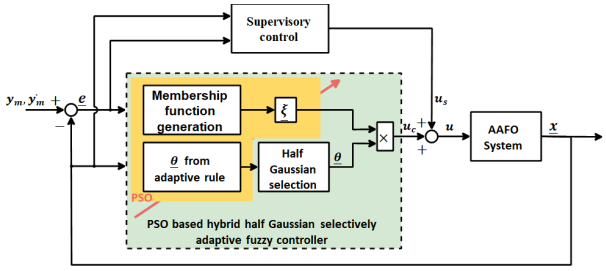

Fig. 2. Architecture of proposed hybrid half-Gaussian selectively adaptive fuzzy controller for actuated ankle–foot orthosis (AAFO). PSO: particle-swarm optimization.

The term $d(t)$ corresponds to the system's nonlinear disturbances; $\xi(t)$ represents the uncertainties due to mass variation, inertia and other AAFO parameters; $B = k_{fv}$; and $C = k_s$.

Thus, let us consider $x_1 = \phi$ and $x_2 = \dot{\phi}$. Then (5) can be re-written as:

$$\begin{aligned} \dot{x_1} &= x_2, \\ \dot{x_2} &= f(x_1, x_2) + b(u + \xi(t) + d(t)), \\ y &= x_1, \end{aligned} \tag{7}$$

where $f(x_1, x_2) = (-Bx_2 - Cx_1)/J$, $b = 1/J$, and the output y is the ankle-joint angle in the saggital plane.

III. Stochastic-Optimization-Based Hybrid Half-Gaussian Selectively Adaptive Fuzzy Control

In the proposed hybrid control scheme (Fig. 2), the structure and free parameters of the fuzzy controller are tuned using PSO; the position of the output singletons of the fuzzy controller are optimized through the use of PSO and a novel HGSA strategy based on Lyapunov stability theory. The details are explained in the following sub-sections.

A. Adaptive fuzzy control strategy: Lyapunov-theory-based approach

The control objective is to compel the ankle-joint angle $\phi = y(t)$ to track a reference trajectory $y_m(t)$. All the closed-loop variables must be bounded to guarantee the stability of the coupled human–AAFO system in the presence of a randomly varying bounded disturbance d(t) and model uncertainties ξ. Let the tracking error be $e = y_m - y$ and the feedback control input be $u = u_c(\underline{x}|\underline{\theta})$, where $\underline{x} = (x_1, x_2, ..., x_n)^T = (x, \dot{x}, ..., x^{(n-1)})^T \in R^n$ is the state vector and $\underline{\theta} = (\theta_1, \theta_2, ..., \theta_N)^T$ is the output singleton vector. The AFLC will ensure adaptation of the parameter vector $\underline{\theta}$ satisfying the following constraints:

Constraint 1: All the variables involved during the operation of the AFLC, i.e., $\underline{x}(t)$, $\underline{\theta}(t)$ and $u(\underline{x}|\underline{\theta})$, must be uniformly bounded: $|\underline{x}(t)| \leq M_x < \infty$, $|\underline{\theta}(t)| \leq M_\theta < \infty$, and $|u(\underline{x}|\underline{\theta})(t)| \leq M_u < \infty$, where M_x, M_θ and M_u are tuned so that the closed-loop system is globally stable in the sense of Lyapunov.

Constraint 2: The closed-loop system must be globally stable in presence of randomly varying bounded uncertainties and disturbances: $|\xi(t)| \leq M_\xi < \infty$, $|d(t)| \leq M_d < \infty$, where M_ξ, M_d are appropriately tuned.

Constraint 3: The tracking error $e(t)$ must be small enough to satisfy Constraint 1 while the vector space $\underline{e} - \underline{\theta}$ should be stable in the sense of Lyapunov for the system.

Let the error vector be $\underline{e} = (e, \dot{e})^T$, and let $\underline{k} = (k_1, k_2)^T$ be chosen so that the roots of the Hurwitz polynomial $k_2 s + k_1$ lie in the left half of the s-plane.

The ideal control law for the system including the disturbances in (7) can be expressed as:

$$u^* = \frac{1}{b}[-f(\underline{x}) + y_m^{(2)} + \underline{k}^T \underline{e}], \tag{8}$$

where $y_m^{(2)}$ is the second derivative of the reference input.

As $f(\underline{x})$ is not accurately known, it is difficult to implement (8) in practice. However, a fuzzy system can be used to approximate the ideal control law. Specifically, the zeroth-order fuzzy Takagi-Sugeno (T-S) system can be used to design the AFLC:

$$u_c(\underline{x}|\underline{\theta}) = \frac{\sum_{l=1}^{\infty} \theta_l * \alpha_l(\underline{x})}{\sum_{l=1}^{\infty} \alpha_l(\underline{x})} = \underline{\theta}^T * \underline{\zeta}(\underline{x}), \tag{9}$$

where $\alpha_l(\underline{x})$, the degree of the lth firing rule, is:

$$\alpha_l(\underline{x}) = \prod_{i=1}^{r} \mu_i^l(x_i). \tag{10}$$

Here, $\mu_i^l(x_i)$ is the membership value of the ith input membership function (MF) in the activated lth rule, r is the number of inputs for the AFLC, $\underline{\zeta}(\underline{x}) = (\zeta_1(\underline{x}), \zeta_2(\underline{x}), ..., \zeta_N(\underline{x}))^T \in R^N$ (where N is the total number of rules) is the normalized firing strength of all IF-THEN rules, and

$$\zeta_l(\underline{x}) = \frac{\alpha_l(\underline{x})}{\prod_{l=1}^{N} \alpha_l(\underline{x})}. \tag{11}$$

The goal is to design an adaptation law for the AFLC that can track the reference trajectory while rejecting the external disturbances and parameter uncertainties. The error dynamics of the system can be expressed as:

$$\begin{aligned} \dot{\underline{e}} =& \underline{\Lambda}_c \underline{e} + \underline{B}_c (\underline{\theta}^* - \underline{\theta})^T \underline{\zeta}(\underline{x}) + \underline{B}_c [u^* - u_c(\underline{x}|\underline{\theta})] \\ & - \underline{B}_c (\xi(t) + d(t)) \end{aligned} \tag{12}$$

where $\underline{\Lambda}_c$ is the error-dynamics system matrix and $\underline{B}_c$ is the error-dynamics input matrix. These correspond to:

$$\underline{\Lambda}_c = \begin{bmatrix} 0 & 1 \\ -k_1 & -k_2 \end{bmatrix} \text{ and } \underline{B}_c = \begin{bmatrix} 0 \\ b \end{bmatrix}. \tag{13}$$

The optimal parameter set can be defined as:

$$\underline{\theta}^* = \arg \min_{\underline{\theta} \in \Re^{\prod_{i=1}^{n} m_i}} \left[\sup_{\underline{x} \in \Re^n} |u^* - u(\underline{x}|\underline{\theta})| \right] \in R^N, \tag{14}$$

where n denotes the dimensionality of the state, and m_i the number of ith firing rules of the fuzzy-logic controller. The error dynamics in (12) can be rewritten as:

$$\dot{\underline{e}} = \underline{\Lambda}_c \underline{e} + b(\underline{\theta}^* - \underline{\theta})^T \underline{\zeta}(\underline{x}) + b[u^* - u_c(\underline{x}|\underline{\theta})] - b\delta(t) \tag{15}$$

where $\delta(t) = \xi_f + \xi(t) + d(t)$ gives the combined effect of the inherent fuzzy-approximation error, model uncertainties, and external disturbances.

Design of supervisory control law for uncertainty and disturbance rejection:

If the disturbances due to the ground reaction forces and uncertainties due to parametric variation of the AAFO system are bounded, then, to ensure state boundedness, the fuzzy control action $u_c(\underline{x}|\underline{\theta})$ should be augmented with a non-fuzzy supervisory-control action $u_s(\underline{x})$ as: $u(t) = u_c(\underline{x}|\underline{\theta}) + u_s(\underline{x})$. It is to be noted here that if the tracking performance of the designed controller is good enough, then it can be easily inferred that the fuzzy approximation error is very small, and thus, $\delta = \xi(t) + d(t)$. Now the closed-loop error dynamics in (12) could be expressed as follows:

$$\begin{aligned}\dot{\underline{e}} =& \underline{\Lambda}_c \underline{e} + b(\underline{\theta}^* - \underline{\theta})^T \underline{\zeta}(\underline{x}) + b[u^* - u_c(\underline{x}|\underline{\theta}) - u_s(\underline{x})] \\ & - b(\xi(t) + d(t))\end{aligned} \tag{16}$$

Let the Lyapunov function for this class of nonlinear system be defined as:

$$V_e = \frac{1}{2}\underline{e}^T \underline{P} \underline{e} + \frac{b}{2\nu}(\underline{\theta}^* - \underline{\theta})^T (\underline{\theta}^* - \underline{\theta}), \tag{17}$$

where ν is the learning rate (a positive constant) and $\underline{P}$ is a symmetric positive definite matrix that satisfies the Lyapunov equation: $\underline{\Lambda}_c^T \underline{P} + \underline{P}\underline{\Lambda}_c = -\underline{Q}$. Q is also a positive definite matrix, and therefore ν in (17) is positive. Therefore, derivative of (17) can be written as:

$$\begin{aligned}\dot{V}_e =& -\frac{1}{2}\underline{e}^T \underline{Q} \underline{e} + \underline{e}^T \underline{P} b[u^* - u_c(\underline{x}|\underline{\theta}) - u_s(\underline{x})] \\ & - \underline{e}^T \underline{P} b \delta(t) + \frac{b}{\nu}(\underline{\theta}^* - \underline{\theta})^T \left[\nu \underline{e}^T P \underline{\zeta}(\underline{x}) - \dot{\underline{\theta}}\right] \\ & \leq -\frac{1}{2}\underline{e}^T \underline{Q} \underline{e} + |\underline{e}^T \underline{P} b| \left(|u^*| - |u_c(\underline{x}|\underline{\theta})|\right) - \underline{e}^T \underline{P} b u_s(\underline{x}) \\ & - \underline{e}^T \underline{P} b \delta(t) + \frac{b}{\nu}(\underline{\theta}^* - \underline{\theta})^T \left[\nu \underline{e}^T P \underline{\zeta}(\underline{x}) - \dot{\underline{\theta}}\right]\end{aligned} \tag{18}$$

Thus, the adaptation law becomes: $\dot{\underline{\theta}} = \nu \underline{e}^T \underline{p}_n \underline{\zeta}(\underline{x})$, where $\underline{p}_n = (p_1, p_2, ..., p_n)^T \in R^N$ is the last column vector of $\underline{P}$.

Now, to make $\dot{V}_e$ a negative semi-definite function, i.e. $\dot{V}_e \leq 0$, $u_s(\underline{x})$ can be written similar to [16] with one extra term for uncertainty as:

$$\begin{aligned}u_s(\underline{x}) =& I_l^* sign\Big(\underline{e}^T \underline{P} b \big[|u_c| + \frac{1}{b_L}(f^U + |y_m^n| \\ & + |\underline{k}^T \underline{e}| - |\xi(t)| - |d(t)|)\big]\Big)\end{aligned} \tag{19}$$

where I_l^* (1, if $V_e > \overline{V}$ and 0, otherwise) determines whether the supervisory control is on or off. $\overline{V}$ is a manually tuned constant. The functions f^U and b_L must obey $f^U > |f(\underline{x})|$ and $0 < b_L \leq b$. As per the Constraint 2, $|\xi(t)| \leq |M_\xi| < \infty$ and $|d(t)| \leq |M_d| < \infty$ should be maintained to ensure the condition $|u| \leq |u_a|$. where u_a is the actuator saturation limit. With the help of $u_s(\underline{x})$ and assuming an active supervisory control (i.e. $I_l^* = 1$) it can be written as:

$$\begin{aligned}\dot{V}_e \leq & -\frac{1}{2}\underline{e}^T \underline{Q} \underline{e} + |\underline{e}^T \underline{P} b| \Big[\frac{1}{b}(|f(x)| + |y_m^n| \\ & + |\underline{k}^T \underline{e}| - |\xi(t)| - |d(t)|)] \\ & - \frac{1}{b_L}(f^U + |y_m^n| + |\underline{k}^T \underline{e}| - |M_\xi| - |M_d|)\Big]\end{aligned} \tag{20}$$

$$\dot{V}_e \leq -\frac{1}{2}\underline{e}^T \underline{Q} \underline{e} \tag{21}$$

Thus, it can be inferred from Lemma 1 and constraint 2 that the external disturbance may be large enough, but bounded one, along with bounded model uncertainties, which is the case for the external disturbances resulting from the rhythmic interaction with the ground. If the fuzzy controller is designed optimally, resulting in minimum approximation error, the closed-loop system will be stable and become robust with respect to the model uncertainties and external disturbances.

Now, as $\underline{Q}$ is positive definite, one can conclude that $\dot{V}_e$ is negative semi-definite, which in turn means $V_e(e(t), \theta(t), \xi(t), d(t)) \leq V_e(e(0), \theta(0), \xi(0), d(0))$, i.e. e, θ, ξ, d are bounded. Let us define $\Phi = \frac{1}{2}\underline{e}^T \underline{Q} \underline{e} \leq -\dot{V}_e$ and integrating Φ with respect to time produces, $\int_0^t \Phi(\lambda)\, d\lambda \leq V_e(0) - V_e(t)$. Hence, $V_e(0)$ is bounded and $V_e(t)$ is monotonically decreasing and bounded. This implies that $\lim_{t\to\infty} \int_0^t \Phi(\lambda)\, d\lambda \leq \infty$. As $\Phi(t)$ is bounded, then utilizing Barbalat's lemma it can be proved that $\lim_{t\to\infty} \Phi(t) = 0$ and thus, $\lim_{t\to\infty} |e(t)| = 0$. Hence, the closed-loop stability is guaranteed along with simultaneous satisfaction of desired tracking performance and uncertainty and disturbance rejection.

B. Hybrid half-Gaussian selectively adaptive fuzzy controller design

AFLCs provide efficient trajectory tracking when time-varying parameters as well as disturbances characterize the system; this is the case for the coupled AAFO–wearer foot system. In the proposed method, the singletons of the fuzzy controller are tuned utilizing PSO [16] within ranges obtained from the Lyapunov stability criteria. Then, they are concurrently adapted, following an adaptation law based on the Lyapunov stability criteria. However, parameter variations requiring such adaptation may not always be present throughout the run time of the system. Adaptation throughout the run time increases the computational burden as well as the required control energy; both are crucial parameters in controller design for rehabilitation-assistive devices, so unnecessary adaptation should be avoided. Thus, in the proposed control strategy, a selection procedure for adaptation is considered: a half-Gaussian probability-density function (PDF) is used to select whether adaptation occurs. When there are disturbances and uncertainties in the system, the error between the reference trajectory and the system output will increase. If the absolute value of the error increases beyond the half-Gaussian PDF curve, adaptation takes place; otherwise, it is not needed. A flowchart of the proposed method is shown in Fig. 3a.

The IAE values of full- and half-Gaussian curves are 1.2150 and 0.8914 rad, respectively. In the full-Gaussian case, the error remains within the curve, and no adaptation takes place (Fig. 3b). For this reason, the half-Gaussian curve is used for selective adaptation in this work. The design procedure of the half-Gaussian curve is elaborated in the next subsection.

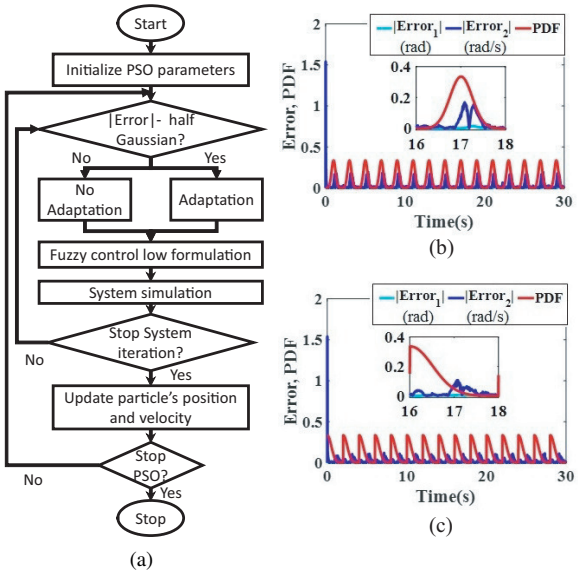

Fig. 3. (a) Flow chart of the proposed hybrid half-Gaussian selectively adaptive fuzzy control strategy. PSO: particle-swarm optimization. (b)–(c): Simulated performance of actuated ankle–foot orthosis system in simulation. Adaptation takes place when magnitudes of position (cyan) and velocity (blue) error exceed (b) full Gaussian and (c) half-Gaussian probability-density function (PDF) curves (red).

Suppose the system runs for a time t_p s. The span of data point is $[-t_p, t_p]$. Let the time step be h. Then, the data points are given as $d_p = -t_p : h : t_p$. Let the mean of the PDF curve be $\mu = 0$, its standard deviation be $\sigma = t_p/4$, and its magnitude be $max(y_m, \dot{y_m})/4$, which is the maximum value of the reference position and the derivative of the curve there. Then the overall full-Gaussian PDF curve is:

$$PDF = \frac{max(y_m, \dot{y_m})}{4} \frac{1}{\sigma\sqrt{2\pi}} e^{\left(\frac{-(d_p-\mu)^2}{2\sigma^2}\right)}. \qquad (22)$$

First a full Gaussian curve for $2t_p$ s will be considered, then a half-Gaussian curve from 0 to t_p s.

Note 1: In the transient state, the error will be relatively high, but it should gradually decline as the steady state is approached. Therefore, at the beginning, high tolerance is allowed for error. Consequently, the Gaussian curve between -t_p s and 0 s is neglected, as it does not allow high error in the transient state. Therefore, from the very beginning, there will be unnecessary adaptation, increasing the required control energy. On the other hand, if the error is not lower in the steady state, it will be higher than one of the Gaussian curves and required adaptation will start. Hence, to provide high error tolerance in the transient state and low error tolerance in the steady state, a half-Gaussian curve is chosen for this proposed method.

Note 2: In the proposed method, the ranges of the parameter values are first obtained from the Lyapunov stability criteria. Then, these ranges are used in the PSO process, which can find the optimal parameters within them. At the same time, the closed-loop system with controller will be stable in the sense of Lyapunov, as the PSO is choosing the parameters within the ranges obtained from the Lyapunov stability criteria. Therefore, the overall proposed method will produce stable, optimal performance. Simulated system performance with the proposed half-Gaussian curve is shown in Fig. 3c, which shows an example of selective adaptation. The proposed controller has been applied to the AAFO hardware system and compared with different existing design strategies in the literature to demonstrate its effectiveness. The experimental description and results are presented and discussed in the next section.

IV. Experimental Results

A. Experimental setup

The orthosis used in this study was an AAFO (AJ-1000, Angel Robotics, South Korea) attached with straps to the subject's left shank and thigh, as shown in Fig. 1b. The orthosis had an active rotational degree of freedom (DoF) at the ankle joint (which was driven by a BLDC motor with a gearbox) and a passive rotational DoF at the knee joint. The joint angle was measured at 1 kHz, using an incremental encoder. The angular velocity of the ankle joint was obtained by taking the time derivative of the angular position numerically and then filtered by a fourth-order lowpass Butterworth filter with a cutoff frequency of 20 Hz. To detect gait-cycle events, three force-sensitive resistors (FSRs) were embedded in both the left and right insoles (a total of six FSRs) and were connected to a wireless FSR-adapter system (Trigono Avanti, Delsys, USA).

B. Experimental protocol

Five healthy subjects (age: 27.6 ± 1.8, height: 175.8 ± 3.1 cm, weight: 67.6 ± 7.3 kg, rest angle: 4.1 ± 2.2°) participated in this experiment. Each subject was informed of the experimental protocols approved by Henri-Mondor Hospital, France, and gave consent before participating in the experiments. They were asked to walk on a treadmill with a set speed of 2 km/h while wearing the AAFO on the left leg. Prior to the experiments, the rest angle was measured for each subject using the AAFO's encoder, and FSR calibration was conducted to normalize FSR values by measuring maximum and minimum values of each FSR sensor during a short period of walking [6].

To validate the tracking performance of the proposed HGSA method, the control performances were compared not only to the unassisted case but also to the performances of a standard tuned proportional–integral–derivative controller (PID), conventional PSO fuzzy controller (PSOF), AFLC, and hybrid fully adaptive fuzzy controller (HFA). Performance was evaluated in terms of ankle-joint position and velocity error, AAFO control input, and adapted fuzzy-output singletons. The comparison methods are described more fully below.

(a). PID: A conventional PID controller was employed. The PID coefficients were set by trial and error to the values P=14, I=12, and D=0.0002.

(b). PSOF: The parameters of the fuzzy controller were obtained from the PSO.
(c). AFLC: The controller was designed utilizing fuzzy adaptive rules obtained from the Lyapunov stability criteria.
(d). HFA: The range of the parameter values to be tuned via PSO was obtained from the Lyapunov stability criteria. First, the parameter values were set by PSO; then they were concurrently adapted following a fuzzy adaptive rule.
(e). HGSA: First the parameter values were set by PSO; then they were adapted following a fuzzy adaptive rule with half-Gaussian selection.

Each control method was implemented using an embedded device (NI myRIO-1900, National Instruments, USA) mounted on the AAFO and running at 1 kHz control frequency. The experiments comprised two sets of six sessions. Each session used one control method and lasted two minutes. The wearers were informed of the experimental protocol, but, to avoid intentional effects on walking performance, they were not told which controller was running in each session. At the end of a session, each participant was asked to sit and rest in a chair for two minutes; after a set of six sessions, 15 minutes rest was given. To analyze the performances in terms of root-mean-square error (RMSE), a zeroth-order TS-type fuzzy controller was designed with a fixed structure configuration of five input MFs for each fuzzified variable (e.g., $N = 25$, $n = 2$, $m_1 = 5$ and $m_2 = 5$ in (14)). The nonlinear dynamics of the system were simulated using a fixed-step fourth-order Runge-Kutta method, with a step size (sampling time) of 0.001 s in conformity with the hardware of the experimental setup. The candidate solution vector (CSV) [18] is obtained from the dynamic coefficients ($J = 0.0252, B = 0.1689$ and $C = 1.0$) in (5) were obtained from system identification method without ground contact. The dynamic model coefficients were considered to be constants derived from the identification process. Hence, the effects of varying these parameters variations were considered to be external perturbations $d(t)$ as an aim to the adaptive control which are included in the human torque variable τ_h. The adaptation gain ν for the adaptive control was set to 0.2, considering the system response.

An online adaptive ankle-reference generator (AARG) scheme was used to generate a tailored ankle-joint kinematic trajectory for each subject. This gait-event-based algorithm generated a desired trajectory in real time by connecting two adjacent key points of the gait cycle using cubic spline functions that were extracted from the gait of 20 healthy subjects [19]. These key points were calculated from ground reaction force measured using FSR sensors. With use of this method, the wearer was not forced to follow a pre-designed trajectory but instead freely chose a trajectory that was automatically updated with respect to wearer speed. (For further information about the AARG scheme, please refer to [6].)

C. Experimental results

As shown in Fig. 4, the continuous reference trajectory generated ankle-joint profiles which were tailored to each subject's walking speed and gait-phase duration. There is no significant difference between the average of gait stride of each subject under five control conditions compared with the unassistance condition ($p > 0.05$). The average ratio of stance phase to entire gait cycle for each subject is observed to be approximately 59%, 64%, 61%, 55%, and 66%. Moreover, The p-values of RMSE for each controller result were evaluated. A significant difference between AFLC and HFA, AFLC and HGSA ($p < 0.01$). The difference between AFLC and None is more significant ($p < 0.001$). However, the difference between AFLC and PID and PSOF is not significant, so on and so forth. It is notable that there is no significant different between HGSA and HFA.

In the terminal-stance and swing phases, the measured ankle-gait trajectories while the AAFO was passive exhibited lower ankle-dorsiflexion angles than the reference trajectory. The maximum error in the terminal-stance phase was 13.36° for subject B; that in the swing phase was 15.79° for subject D. Hence, considering that the direction of the torque coincided with the ankle-angle direction (i.e., positive torque was dorsiflexion and negative torque was plantarflexion), the positive torque during the stance phase was provided by the AAFO to the ankle. Subject B's result showed the largest improvement of the dorsiflexion angle: the error was reduced by 79.79%, as shown in Fig. 4b. At the end of the pre-swing phase, the plantarflexion torque was provided by the AAFO for push-off assistance over a relatively short time, even when the measured ankle angle had a higher plantarflexion angle than the reference angle, as notably shown in Fig. 4a and 4d. During the swing phase, dorsiflexion assistance was provided by the AAFO to all participants to help clearance of the foot. Fig. 4d shows that the best error reduction during the swing phase was 94.15%. For each experimental subject, the proposed controller produced similar torque behavior and trajectory-tracking performance.

The average RMS angular position and velocity errors of the six controllers during experiments with five healthy subjects are summarized in Table I. For all control strategies, tracking errors were smaller when the assistive torque was provided to the coupled human–AAFO system. In the case of the PID controller, the position error was low ($3.29 \pm 0.44°$), but the velocity error was high ($35.81 \pm 5.78°/s$). PSOF did not reduce the position error as much as the other methods, although it produced better results in terms of the velocity error ($28.95 \pm 3.22°/s$) than PID or AFLC. The performance of HFA (position error $2.81 \pm 0.51°$ and velocity error 28.02 $\pm$ $3.95°/s$) was better than that of PID, PSOF, or AFLC. However, the proposed HGSA controller showed the best tracking performance in terms of both position error ($2.81 \pm 0.47°$) and velocity error ($27.01 \pm 3.25°/s$).

As shown in Fig. 5a, using the proposed control strategy improved the tracking performance. This is clearly seen by comparing the average tracking-error-reduction rate to that for the unassisted session. The tracking performances of PID, PSOF, and AFLC were not satisfactory. By contrast, in the cases of HFA ($54.69 \pm 14.02\%$) and proposed HGSA ($54.33 \pm 14.67\%$), the tracking performances were much better. Though HFA and HGSA provided similar tracking performances, the

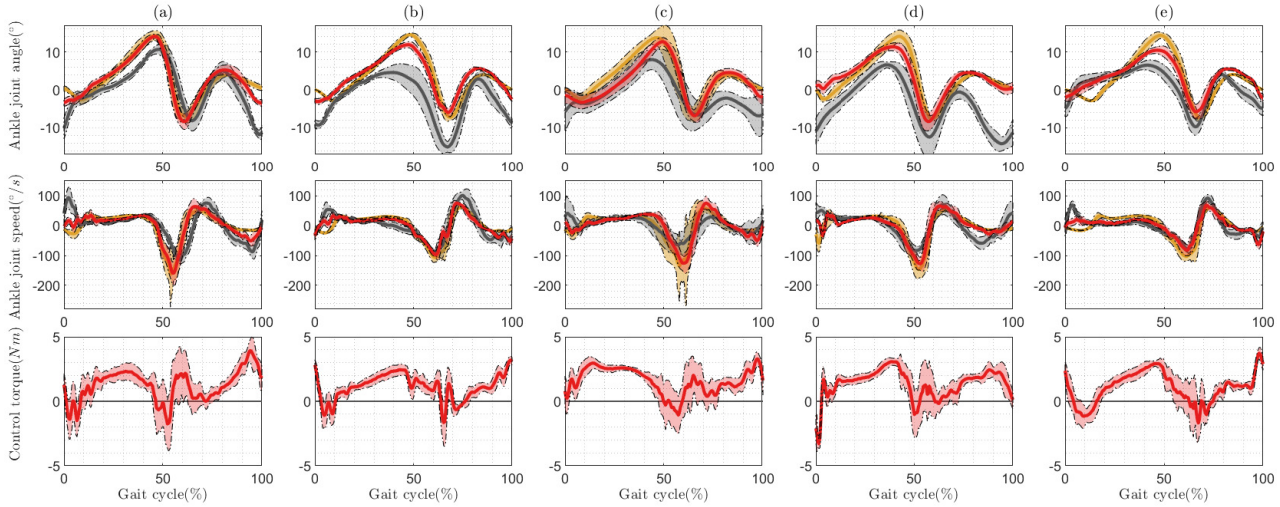

Fig. 4. Average ankle angular position, velocity, and control torque (± standard deviation) for each subject over the gait cycle. The yellow line represents the desired profile, the red line represents the measured profile with the proposed method, and the black line represents the measured profile without assistance. The data were extracted from the sessions between 100—120 s, normalized with respect to 100% gait cycle, and interpolated over 200 samples using a spline function. The control input direction was the same as that of the ankle-joint angle.

TABLE I
PERFORMANCE OF DIFFERENT CONTROLLERS IN EXPERIMENTS WITH HUMAN SUBJECTS

Subject	Control strategy (RMS postion error, unit : °)					
	Un[†]	PID	PSOF	AFLC	HFA	HGSA
mean(A, A*)	5.16	3.26	3.50	3.68	2.29	2.54
mean(B, B*)	7.34	2.70	3.68	3.09	2.45	2.31
mean(C, C*)	5.45	3.06	3.14	3.22	2.75	2.79
mean(D, D*)	9.22	3.84	5.30	3.57	2.96	2.85
mean(E, E*)	5.42	3.56	3.93	3.68	3.60	3.56
mean(All[‡])	6.52	3.29	3.91	3.45	2.81	2.81
Std(All[‡])	1.74	0.44	0.83	0.28	0.51	0.47
Subject	Control strategy (RMS velocity error, unit : °/s)					
	Un[†]	PID	PSOF	AFLC	HFA	HGSA
mean(A, A*)	47.58	43.62	32.18	42.50	33.67	31.45
mean(A, A*)	34.77	28.23	24.07	31.63	22.58	22.31
mean(C, C*)	42.99	38.74	27.60	34.24	27.28	27.17
mean(D, D*)	45.95	35.15	31.10	31.62	27.99	26.62
mean(E, E*)	35.54	33.31	29.77	33.11	28.59	27.50
mean(All[‡])	41.37	35.81	28.95	34.62	28.02	27.01
Std(All[‡])	5.91	5.78	3.22	4.54	3.95	3.25

[*]: *Session separator*, [†]: *Unassisted session*, [‡]: *All subjects*

selective adaptation used by HGSA required less control signal than the full adaptation used by HFA (Obviously, the other three methods required even less control signal, but this advantage was offset by their poor tracking performance.), as shown in Fig. 5b. In the case of the proposed HGSA method, output singletons were selectively adapted to reduce the computational effort. During the experiments, the adaptation law was in effect only when the position and velocity errors were above the PDF curve. Hence, for each subject, the adaptation was selectively executed during only 63.5 ± 2.67% of the time compared to the full adaption method. The transient performance of HGSA is shown in Fig. 6.

Improving ankle dorsiflexion with few degrees during the swing phase duration could have a great impact on the patient

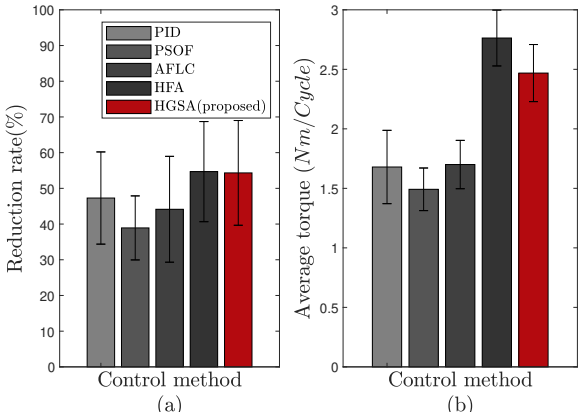

Fig. 5. Mean and standard deviation of the performance of each control method: (a) The reduction rate of root-mean-square error throughout each gait cycle. (b) The torque integration throughout each gait cycle.

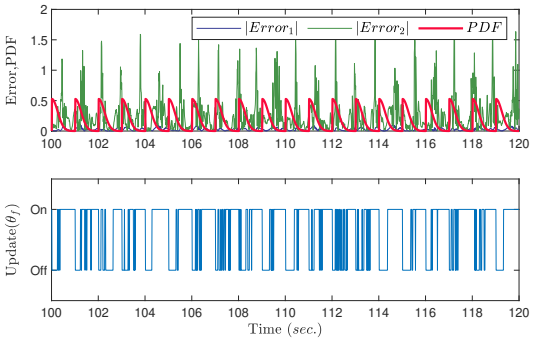

Fig. 6. Performance of the proposed method during 100—120 s portion of experimental session. (a) Adaptation takes place when magnitude of position (blue) or velocity (green) error exceeds half-Gaussian probability-density function (PDF) curve (red). (b) Switching update of proposed method.

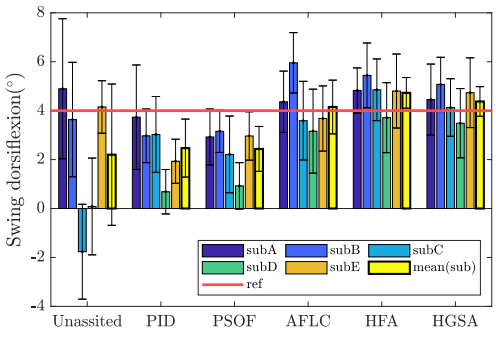

Fig. 7. Maximum dorsiflexion (MD) during swing phase of walking. Data re-sampled over 200 data point for full gait cycle and calculated the maximum dorsiflexion angle during swing phases. red bold line represents the reference maximum dorsiflexion. Respectfully, the box plot showed the mean of MD($\pm$ standard deviation) at each control method

as this would considerably limits the fall risks. Therefore, Fig. 7 is focused on the maximum dorsiflexion (MD) that could be achieved with the proposed strategy during swing phase. It is noteworthy that the proposed controller showed the closest angle with respect to the reference angle with the average angle of different subjects as $4.38 \pm 0.61°$.

V. Conclusion

In this paper, a hybrid HGSA logic controller is proposed for control of a nonlinear wearable AAFO during walking. Fuzzy singletons are at first selected by PSO and then concurrently adapted to cope with time-varying uncertainties and disturbances present in the system. To reduce the required control energy, the adaptation only takes place when the magnitude of the tracking error exceeds a certain half-Gaussian function. The performance of the proposed method was verified in both simulation and real-time experiments. For the latter, the reference trajectory was designed by an online adaptive method able to generate an ankle-joint profile tailored to each subject's walking speed and gait phase duration. Only ground-reaction forces were used, making the system portable. Finally, stable tracking performance was observed for all five participants, and less energy was required to ensure satisfactory trajectory tracking than in standard control techniques. The results show that an adaptive ankle-reference profile generated in real-time based on the current state of the wearer's gait could potentially assist the ankle joint and, if the wearer is a paretic patient, prevent eventual falls due to foot-drop effects by increasing ankle dorsiflexion during the swing phase (which can correct foot drop even in the presence of co-contraction) and plantarflexion during push-off.

References

[1] J. D. Stewart, "Foot drop: where, why and what to do?" *Practical neurology*, vol. 8, no. 3, pp. 158–169, 2008.

[2] P. K. Jamwal, "Design analysis and control of wearable ankle rehabilitation robot," Ph.D. dissertation, University of Auckland, 2011.

[3] C. A. Coste, J. Jovic, R. Pissard-Gibollet, and J. Froger, "Continuous gait cycle index estimation for electrical stimulation assisted foot drop correction," *Journal of neuroengineering and rehabilitation*, vol. 11, no. 1, p. 118, 2014.

[4] M. Noël, B. Cantin, S. Lambert, C. M. Gosselin, and L. J. Bouyer, "An electrohydraulic actuated ankle foot orthosis to generate force fields and to test proprioceptive reflexes during human walking," *IEEE Transactions on Neural Systems and Rehabilitation Engineering*, vol. 16, no. 4, pp. 390–399, 2008.

[5] J. A. Blaya and H. Herr, "Adaptive control of a variable-impedance ankle-foot orthosis to assist drop-foot gait," *IEEE Transactions on neural systems and rehabilitation engineering*, vol. 12, no. 1, pp. 24–31, 2004.

[6] V. Arnez-Paniagua, H. Rifaï, Y. Amirat, M. Ghedira, J. Gracies, and S. Mohammed, "Adaptive control of an actuated ankle foot orthosis for paretic patients," *Control Engineering Practice*, vol. 90, pp. 207–220, 2019.

[7] M. J. Lawn, M. Takashima, M. Ninomiya, J. Yu, K. Soma, and T. Ishimatsu, "Development of an actuation system for a rotary hydraulic brake on a low cost light weight knee-ankle-foot orthosis," in *2015 IEEE SENSORS*. IEEE, 2015, pp. 1–4.

[8] W. Huo, S. Mohammed, and Y. Amirat, "Impedance reduction control of a knee joint human-exoskeleton system," *IEEE Transactions on Control Systems Technology*, vol. 27, no. 6, pp. 2541–2556, 2018.

[9] M. Zhang, J. Cao, S. Q. Xie, G. Zhu, X. Zeng, X. Huang, and Q. Xu, "A preliminary study on robot-assisted ankle rehabilitation for the treatment of drop foot," *Journal of Intelligent & Robotic Systems*, vol. 91, no. 2, pp. 207–215, 2018.

[10] J. Guerrero-Castellanos, H. Rifaï, V. Arnez-Paniagua, J. Linares-Flores, L. Saynes-Torres, and S. Mohammed, "Robust active disturbance rejection control via control lyapunov functions: Application to actuated-ankle–foot-orthosis," *Control Engineering Practice*, vol. 80, pp. 49–60, 2018.

[11] N. Wang and M. J. Er, "Direct adaptive fuzzy tracking control of marine vehicles with fully unknown parametric dynamics and uncertainties," *IEEE Transactions on Control Systems Technology*, vol. 24, no. 5, pp. 1845–1852, 2016.

[12] R. Maiti, K. D. Sharma, and G. Sarkar, "Linear consequence-based fuzzy parallel distributed compensation type l_1 adaptive controller for two link robot manipulator," *IEEE Transactions on Circuits and Systems I: Regular Papers*, vol. 66, no. 10, pp. 3978–3990, 2019.

[13] S.-M. Chen and C.-H. Chiou, "Multiattribute decision making based on interval-valued intuitionistic fuzzy sets, pso techniques, and evidential reasoning methodology," *IEEE Transactions on Fuzzy Systems*, vol. 23, no. 6, pp. 1905–1916, 2014.

[14] J. Wang and T. Kumbasar, "Parameter optimization of interval type-2 fuzzy neural networks based on pso and bbbc methods," *IEEE/CAA Journal of Automatica Sinica*, vol. 6, no. 1, pp. 247–257, 2019.

[15] S.-M. Chen and W.-C. Hsin, "Weighted fuzzy interpolative reasoning based on the slopes of fuzzy sets and particle swarm optimization techniques," *IEEE Transactions on Cybernetics*, vol. 45, no. 7, pp. 1250–1261, 2014.

[16] K. D. Sharma, A. Chatterjee, and A. Rakshit, "A hybrid approach for design of stable adaptive fuzzy controllers employing lyapunov theory and particle swarm optimization," *IEEE Transactions on Fuzzy Systems*, vol. 17, no. 2, pp. 329–342, 2009.

[17] K. D. Sharma, A. Chatterjee, P. Siarry, and A. Rakshit, "A novel disturbance rejection factor based stable direct adaptive fuzzy control strategy for a class of nonlinear systems," *Expert Systems*, vol. 38, no. 3, pp. 1–23, 2020.

[18] K. D. Sharma, A. Chatterjee, and A. Rakshit, "Harmony search algorithm and lyapunov theory based hybrid adaptive fuzzy controller for temperature control of air heater system with transport-delay," *Applied Soft Computing*, vol. 25, pp. 40–50, 2014.

[19] E. Hutin, D. Pradon, F. Barbier, B. Bussel, J.-M. Gracies, and N. Roche, "Walking velocity and lower limb coordination in hemiparesis," *Gait & posture*, vol. 36, no. 2, pp. 205–211, 2012.